International Journal of Mass Spectrometry 300 (2011) 108–117

Contents lists available at ScienceDirect

International Journal of Mass Spectrometry

journal homepage: www.elsevier.com/locate/ijms

The role of proton bridges in selective cleavage of Ser-, Thr-, Cys-, Met-, Asp-, and Asn-containing peptides

Qingfen Zhang[1], Brittany Perkins[2], Guanhong Tan[3], Vicki H. Wysocki*

Department of Chemistry and Biochemistry, University of Arizona, Tucson, AZ 85721, USA

ARTICLE INFO

Article history:
Available online 13 October 2010

Keywords:
Mass spectrometry
ESI
Peptide fragmentation
Proton bridge
Molecular modeling

ABSTRACT

Fragmentation patterns of doubly charged peptides containing serine (Ser), threonine (Thr), cysteine (Cys), homoserine (Hse), methionine (Met), aspartic acid (Asp), or asparagine (Asn) and terminating with arginine (Arg) were investigated. Stronger cleavages N-terminal to Ser, Thr, Cys, Asp, and Asn were observed in comparison to their C-terminal cleavages. In contrast, stronger cleavages C-terminal to Hse and Met were observed compared to their N-terminal cleavages. These fragmentation patterns can be explained by the relative stabilities of intramolecular proton bridges that form between the side chain heteroatoms (hydroxyl oxygen, carbonyl oxygen or sulfur) and the neighboring backbone carbonyl oxygens. Literature data and results from molecular dynamics are used to explain the stabilities of the proton bridges with different ring sizes based on the site of the bridge. For Ser, Thr, Cys, Asn and Asp, the proton bridge between the side chain and the adjacent N-terminal carbonyl is more stable and thus favored over the one to the adjacent C-terminal carbonyl, resulting in N-terminal enhanced cleavage. For Met and Hse, the proton bridge between the side chain and the C-terminal carbonyl is more stable, leading to C-terminal enhanced cleavages.

1. Introduction

Mass spectrometry is a leading technology for proteomics and bioscience research in the current postgenomic era. The great improvements in mass spectrometry over the last two decades have revolutionized the analysis of proteins and peptides. These improvements include the advent of the soft ionization methods electrospray ionization (ESI) [1] and matrix-assisted laser desorption/ionization (MALDI) [2,3], the availability of diverse instruments [4–10], and the development of various dissociation methods [11–14]. The process of automated high throughput peptide sequencing and protein identification by mass spectrometry results in massive amounts of MS/MS data. The use of computer algorithms was pioneered by Henzel, Watanabe, and Stults [15,16] and continued by Yates et al. [17] and Mann et al. [18], among others, and has allowed for the fast analysis necessary to handle the data output. This is achieved by correlating the experimental peptide spectra or peak lists with those of theoretical peptides generated from 'in silico' digests of proteins and translated DNA databases. Algorithms such as SEQUEST [19] and MASCOT [20] incorporate some current knowledge regarding peptide fragmentation gained from applied and fundamental research and have proved highly useful. However, these and other current algorithms such as X!Tandem [21,22], OMSSA [23], and Phenyx [24] give only limited weight to the different chemical properties of amino acids and their effects on peptide dissociation in the gas phase. The utility of current algorithms might be enhanced if more rules governing peptide fragmentation are explored and appropriately incorporated into identification algorithms. Improving our current knowledge of peptide fragmentation through a better understanding of enhanced cleavage is thus highly desired.

Under most circumstances, fragment ions from MS/MS of peptides are generated by charge-directed cleavages. According to the mobile proton model [11,25–28], the ionizing proton is sequestered by a basic site (e.g. the N-terminal amine group or the side chains of basic residues) and cleavages are initiated after the ionizing proton is transferred intramolecularly to heteroatoms along the peptide backbone. It is also widely accepted that the ionizing proton tends to be intramolecularly "solvated" by multiple heteroatoms in a peptide in the gas phase [29]. Many other factors can also affect peptide unimolecular dissociation in the gas phase, including peptide length [30], charge state and the number of basic residues [25,31], energy deposition and the instrument time frame [31,32], chemical properties of amino acids in the sequence [25,33–35], and the secondary structure [25] of a peptide formed by a given amino acid

* Corresponding author. Tel.: +1 520 621 2628; fax: +1 520 621 8407.
E-mail address: vwysocki@u.arizona.edu (V.H. Wysocki).
[1] Current address: Sanofi-Aventis, Tucson, AZ, USA.
[2] Current address: University of New Mexico, Albuquerque, NM, USA.
[3] Current address: Amgen, Thousand Oaks, CA, USA.

1387-3806/$ – see front matter © 2010 Elsevier B.V. All rights reserved.
doi:10.1016/j.ijms.2010.09.025

sequence. Peptides that give uniform (nonselective) cleavages can be sequenced more readily because a full series of b ions and/or y ions are usually generated and algorithms are often written to favor contiguous series. In contrast, selective cleavages may make peptide sequencing troublesome by only giving strong cleavages at certain amino acids. It has been observed that selective cleavages dominate in the presence of certain amino acids. For example, if Asp is present in a peptide, cleavage C-terminal to Asp is preferential if the ionizing proton is sequestered by a basic residue (e.g. arginine) [35–37], cleavage C-terminal to histidine is favored by protonation at His [34] and cleavage N-terminal to proline is enhanced by the presence of at least one mobile proton [37,38]. These studies not only benefit peptide sequencing and protein identification, but also improve our general understanding of the unimolecular dissociation process in the gas phase.

This study investigates the role of proton bridges in initiating enhanced cleavage within peptides containing serine (Ser), threonine (Thr), cysteine (Cys), methionine (Met), homoserine (Hse), aspartic acid (Asp) and asparagine (Asn). Recently, it was found by data mining of a large set of doubly charged peptide MS/MS spectra that cleavages N-terminal to Ser and Thr are slightly enhanced compared to cleavages C-terminal to these residues [37,39,40]. This specific cleavage pattern of Ser and Thr has already been noticed by other researchers and incorporated into a de novo sequencing algorithm, Pepnovo [41]. Because the side chains of Cys, Met, and Hse can also interact with backbone carbonyl groups via their heteroatoms, studying these residues may help elucidate the mechanism for enhanced cleavage. The side chain of Asp can attack a backbone carbonyl and cause enhanced C-terminal cleavage when the ionizing proton is not involved [35,36], but in this paper we report that cleavage N-terminal to Asp is enhanced when a mobile proton is present. In the case of Asn, a suppressed cleavage at its C-terminal side was observed for doubly charged Asn-containing peptides [37], but the cause has not been studied. In order to further understand and explain these observations, a series of Arg-containing doubly charged peptides containing the residues of interest were fragmented in an ion trap mass spectrometer. The interaction of backbone carbonyls and side chains through proton bridges and the effect of the bridge on spectral appearance were probed by examining the fragmentation patterns and calculating the stability of the resulting proton bridges.

2. Experimental methods

2.1. Peptide synthesis

The synthetic peptides used were prepared using multiple solid-phase synthesis protocols outlined by Atherton and Sheppard [42]. The 9-fluoroenylmethoxycarbonyl (Fmoc) derivatives of several required amino acids (Fmoc-L-alanine, Fmoc-L-glycine and Fmoc-*O*-*tert*-butyl-L-threonine) were purchased from Advanced Chemtech (Louisville, KY). Fmoc derivatives of other amino acids (Fmoc-*O*-*trityl*-L-homoserine, Fmoc-*O*-*tert*-*butyl*-L-serine, Fmoc-*O*-*tert*-*butyl*-D-serine, Fmoc-*S*-*trityl*-L-cysteine,) were purchased from Novabiochem (La Jolla, CA). Fmoc-*S*-*methyl*-L-cysteine was purchased from Bachem (Torrance, CA). The C-terminal residues required for peptide synthesis were purchased already attached to resins (Fmoc-pentamethylchroman(PMC)-Arg-Wang resin) from Advanced Chemtech (Louisville, KY). All other reagents required during synthesis were from Aldrich (Milwaukee, WI). Removal of Fmoc during the synthesis was performed using piperidine (20%) in dimethylformamide (DMF). Coupling reactions between successive L-amino acid residues were performed in a solution of DMF containing 2-fold molar excess N-hydroxybenzotriazole dihydrate (HOBt) and benzotriazole-1-yl-oxy-Tris-(dimethyamino)-phosphonium hexafluorophosphate (BOP; Castro's reagent), 4-fold molar excess of diisopropylethylamine (DIEA), and the appropriate Fmoc-protected amino acids. The synthesized peptides were cleaved from the resin and deprotected using a mixture of 95% trifluoroacetic acid (TFA), 2.5% H_2O and 2.5% triisopropylsilane (TIPS) for 1.5 h at ambient temperature.

2.2. Ions used to analyze fragmentation patterns

For protonated peptides activated by collisions with gas, the most common fragment ions are formed upon cleavages at amide bonds along the peptide backbone: the resulting ions are b ions if the N-terminal fragments retain the charge after the cleavage, y ions if the C-terminal fragments retain the charge. The structures of b and y ions have been well studied. The most common structure for b ions has been suggested to be an oxazolone structure [43–46] and for y ions truncated peptides, with large macrocyclic b ions also possible [47]. The ions 28 amu lower in mass than b ions are designated as a-type ions; other types of fragment ions are immonium ions, the ions formed upon side chain cleavages (d, v, w ions) and the ions generated from various neutral losses (the loss of NH_3, H_2O, etc.) [14,48,49].

2.3. Collision-induced dissociation (CID)

Low energy CID experiments were performed with a ThermoFinnigan LCQ ion trap mass spectrometer. The peptides were dissolved in a solution of H_2O:CH_3CN (1:1, v/v) containing 5% TFA and 0.5–0.7% *m*-nitrobenzyl alcohol to a concentration of 20–30 pmol/μL. The use of *m*-NBA and the relatively high concentration of TFA are to obtain doubly charged ions with appropriate intensities [50]. The peptide solutions were then sprayed into the mass spectrometer at a rate of 3–8 μL/min. The applied needle voltage was 4 kV and the capillary temperature was maintained at 200 °C for all samples. Helium was used as the collision gas, and the excitation energy is indicated as % collision energy (range for experiments = 25–70%) by the manufacturer and corresponds to the amplitude of a supplementary AC voltage that is adjusted to eliminate the *m*/*z*-dependent fragmentation of the precursor ions.

2.4. Molecular modeling

The model structures containing amino acids of interest were built in MacroModel (version 8.1) using the built-in amino acid library. The model structures were modified to carry a positive charge (proton) with the charge being placed on a selected carbonyl or hydroxyl oxygen. The protonated built-in structure was first subjected to a conformational search resulting in a series of stable conformers. The conformational search was performed with the Monte Carlo mixture model (MCMM) using the Merck molecular force field (MMFF), and the default structural parameters were used for a conformational search with 1000 minimization steps and 1000 iterations. The most stable conformer containing the proton bridge of interest was subjected to molecular dynamics using the MMFF force field. MMFF force field default parameters were used for the electrostatic and hydrogen bonding treatments during molecular dynamics. The Polak–Riviere conjugate gradient (PRCG) was used for the energy minimization routines both for molecular dynamics and for conformational searches. In all, 10,000 structures were sampled during the molecular dynamic run (1 fs time step; 10 ps total time; initial and final temperatures were the same; 0.5 ps bath time).

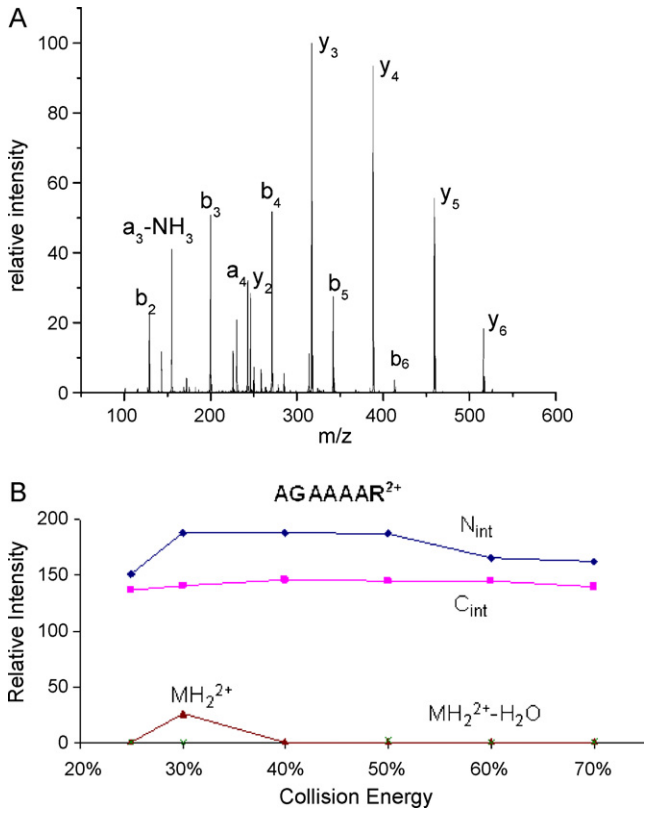

Fig. 1. (A) CID spectrum of the doubly charged AGAAAAR (*m*/*z*: 294) by ESI/LCQ. The "% relative collision energy" (defined by the instrument manufacturer) used for acquiring the spectrum was 50%. (B) Relative intensity curve of doubly charged AGAAAAR LCQ/ESI. N_{int}: the intensity sum of fragments corresponding to cleavage N-terminal to the Ala in the fourth position including y_4, b_3 and its secondary fragments (a_3 and a_3-NH_3) if observed. C_{int}: the intensity sum of fragments C-terminal to Ala in the fourth position, including y_3, b_4 and its secondary fragments (a_4 and a_4-NH_3) if observed. No obvious secondary fragmentation of y ions is observed.

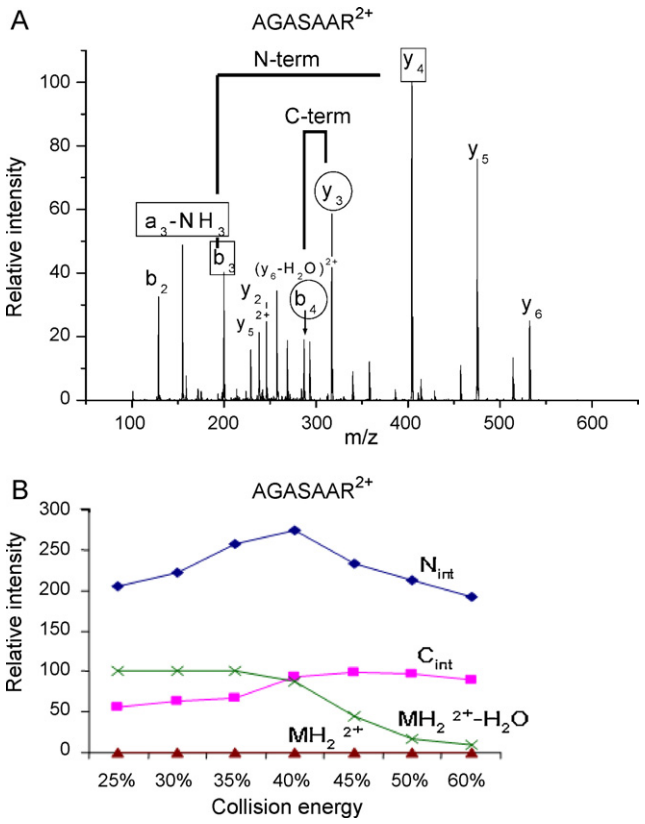

Fig. 2. (A) CID spectrum by ESI/LCQ of doubly charged AGASAAR (*m*/*z*: 302). The "% relative collision energy" (defined by the instrument manufacturer) used for acquiring the spectrum was 50%. Circles denote fragments C-terminal to Ser and rectangles denote fragments N-terminal to Ser. (B) Relative intensity curve of doubly charged AGASAAR LCQ/ESI. N_{int}: the intensity sum of fragments N-terminal to Ser including y_4, b_3 and its secondary fragments (a_3 and a_3-NH_3) if observed. C_{int}: the intensity sum of fragments C-terminal to Ser, including y_3, b_4 and its secondary fragments (a_4 and a_4-NH_3) if observed. No obvious secondary fragmentation of y ions is observed.

3. Results and discussion

3.1. Model peptides

Model peptides are commonly used to study peptide fragmentation because this allows systematic substitution of amino acid residues [34] and modification of the N- or C-terminus [51,52]. This strategy was used in the present study to investigate the specific fragmentation patterns of peptides containing Ser, Thr, Cys, Met, Hse (homoserine), Asn, and Asp. After comparing fragmentation of several model peptide candidates, the model peptide AGA**X**AAR was chosen for the present study, where X represents the amino acid of interest. The major reason for choosing AGA**X**AAR as the model peptide is the uniform cleavage observed for doubly charged AGA**A**AAR (where X represents Ala) (Fig. 1). AGA**A**AAR can be used as a control peptide to identify any selective fragmentation patterns induced by amino acid X by comparing the fragmentation of AGA**A**AAR and AGA**X**AAR. It was desirable to have at least one Gly in the sequence to avoid helix formation. Although Gly is typically predicted to have enhanced cleavages at its N-terminus by statistical analysis, this is avoided by placement of Gly as the second residue. The typical enhanced cleavage N-terminal to Gly is prevented presumably because its position as the second residue in the sequence means that there is no preceding carbonyl to attack the carbonyl N-terminal to Gly. Doubly charged ions were investigated, assuming that one proton will localize at the basic Arg side chain [25] allowing the second proton to be "mobile" to initiate charge-directed cleavage.

3.2. Fragmentation data

Ser, Thr, and Cys each have a similar side chain structure consisting of a β-carbon atom bonded to an electronegative heteratom. Doubly charged AGA**X**AAR (X = Ser, Thr, Cys) were fragmented to probe the effect of these amino acids on fragmentation patterns. In contrast with the CID spectra of doubly charged AGA**A**AAR, the CID spectra of doubly charged AGA**S**AAR, AGA**T**AAR, and AGA**C**AAR exhibit enhanced cleavages N-terminal to the Ser, Thr, and Cys, respectively. The spectrum for the Ser-containing peptide is shown in Fig. 2A. The extent of cleavage enhancement is determined by comparing the intensity of the fragments corresponding to cleavage N-terminal to the amino acid in question (y_4, b_3, a_3 and a_3-NH_3 if observed) relative to the fragments corresponding to cleavage C-terminal to the amino acid (y_3, b_4, a_4 and a_4-NH_3 if observed). The plot of relative intensity as a function of collision energy for doubly charged AGA**S**AAR is shown in Fig. 2B. The plot shows a higher total intensity of the fragments corresponding to N-terminal cleavage compared with fragments corresponding to C-terminal cleavage. The other two peptides showed similar trends (data not shown). The enhanced cleavage N-terminal to Ser and Thr is consistent with the trend predicted by statistical analysis of large data sets [37,39,53] (Cys was depleted in the PNNL dataset so no trend was predicted).

The lower intensity of y_3 (C-terminal cleavage) compared to y_4 (N-terminal cleavage) could be a result of further fragmentation of y_3 during the experiment, causing a decrease in the y_3 peak, so MS^3 was performed to explore this possibility. MS^3 of the y_3 peak

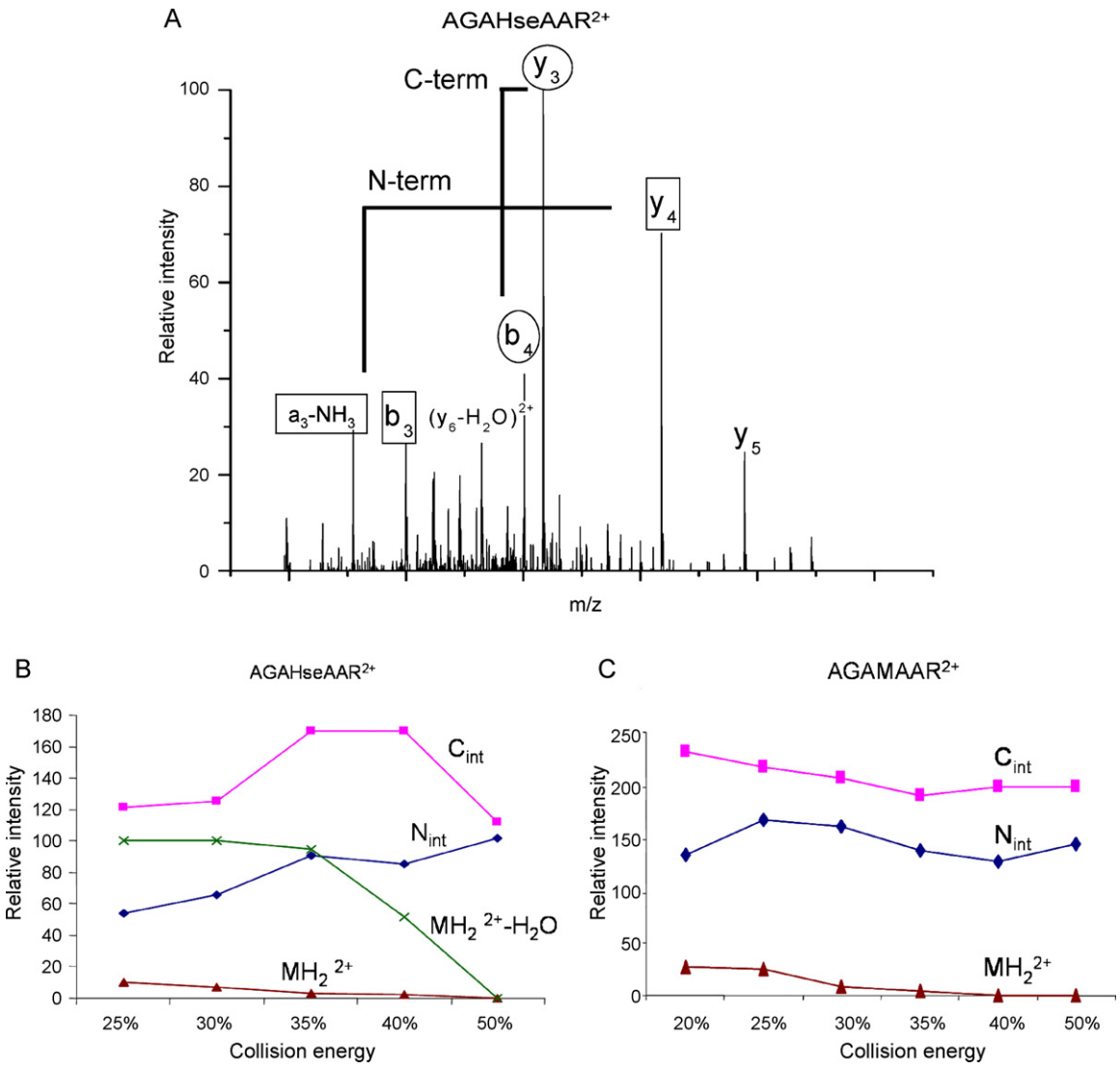

Fig. 3. (A) CID spectrum by ESI/LCQ of doubly charged AGAHseAAR (m/z: 309). The "% relative collision energy" (defined by the instrument manufacturer) used for acquiring the spectrum was 50%. Circles denote fragmentation C-terminal to Hse and rectangles denote fragmentation N-terminal to Hse. Relative intensity curves of doubly charged (B) AGAHseAAR and (C) AGAMAAR by LCQ/ESI. N_{int}: the intensity sum of fragments N-terminal to Hse/Met including y_4, b_3 and its secondary fragments (a_3 and a_3-NH_3) if observed. C_{int}: the intensity sum of fragments C-terminal to Hse/Met, including y_3, b_4 and its secondary fragments (a_4 and a_4-NH_3) if observed. No obvious secondary fragmentation of y ions is observed.

showed prominent secondary fragments such as y_1 and y_3-NH_3-H_2O; these peaks, however, were not prominent in the MS/MS of the original precursor. These secondary y_3 fragment peaks are not evident in any of the three MS/MS spectra for Ser, Thr, and Cys, so it can be concluded that the lower intensity of y_3 is caused by the suppressed cleavage C-terminal to these residues.

Hse and Met were also studied to determine if side chain length played a role in fragmentation patterns. Hse is a serine analogue that contains one additional methylene group in the side chain. Met is a natural amino acid similar to cysteine which contains one more methylene group in the side chain; the sulfur also has a methyl group attached instead of hydrogen. In contrast to the N-terminal enhanced cleavage patterns demonstrated by the other amino acids, doubly charged AGA**Hse**AAR demonstrates C-terminal enhanced cleavage as shown in Fig. 3A; AGA**M**AAR^{+2} showed similar results. The ion y_3 corresponding to cleavage C-terminal to Hse yields one of the most prominent peaks and y_3 is higher in intensity than the N-terminal fragment y_4. The relative intensity curves also show C-terminal enhanced cleavage across collision energies ranging from 25% to 50% for AGA**Hse**AAR and AGA**M**AAR (Fig. 3B and C). In contrast, the similar plot for AGA**S**AAR (Fig. 2B) shows dominant N-terminal cleavage.

The side chains of Asn and Asp also contain heteroatoms in the form of an amide and carboxylic acid group, respectively. Some research has already been done on the fragmentation patterns for these two amino acids. Statistical analysis has shown that cleavages N-terminal to Asn are stronger than those C-terminal to Asn for doubly charged tryptic peptides [37]. For Asp, it is well known that enhanced cleavages C-terminal to Asp occur for peptides without a mobile proton, e.g., for singly charged Arg-containing peptides [35–37,39]. There are no reported fragmentation patterns for peptides containing Asp and a mobile proton besides the disappearance of C-terminal enhanced cleavage. The doubly charged model peptides AGA**N**AAR and AGA**D**AAR containing Asn or Asp were fragmented; the spectra are shown in Fig. 4A and B. Similar to Ser, Thr, and Cys, the spectra show enhanced N-terminal fragments and suppressed C-terminal cleavage. The relative intensity curves for doubly charged AGA**N**AAR and AGA**D**AAR show N-terminal enhanced cleavages across collision energies ranging from 18% to 40% (Fig. 4C and D). Again, no additional peaks from

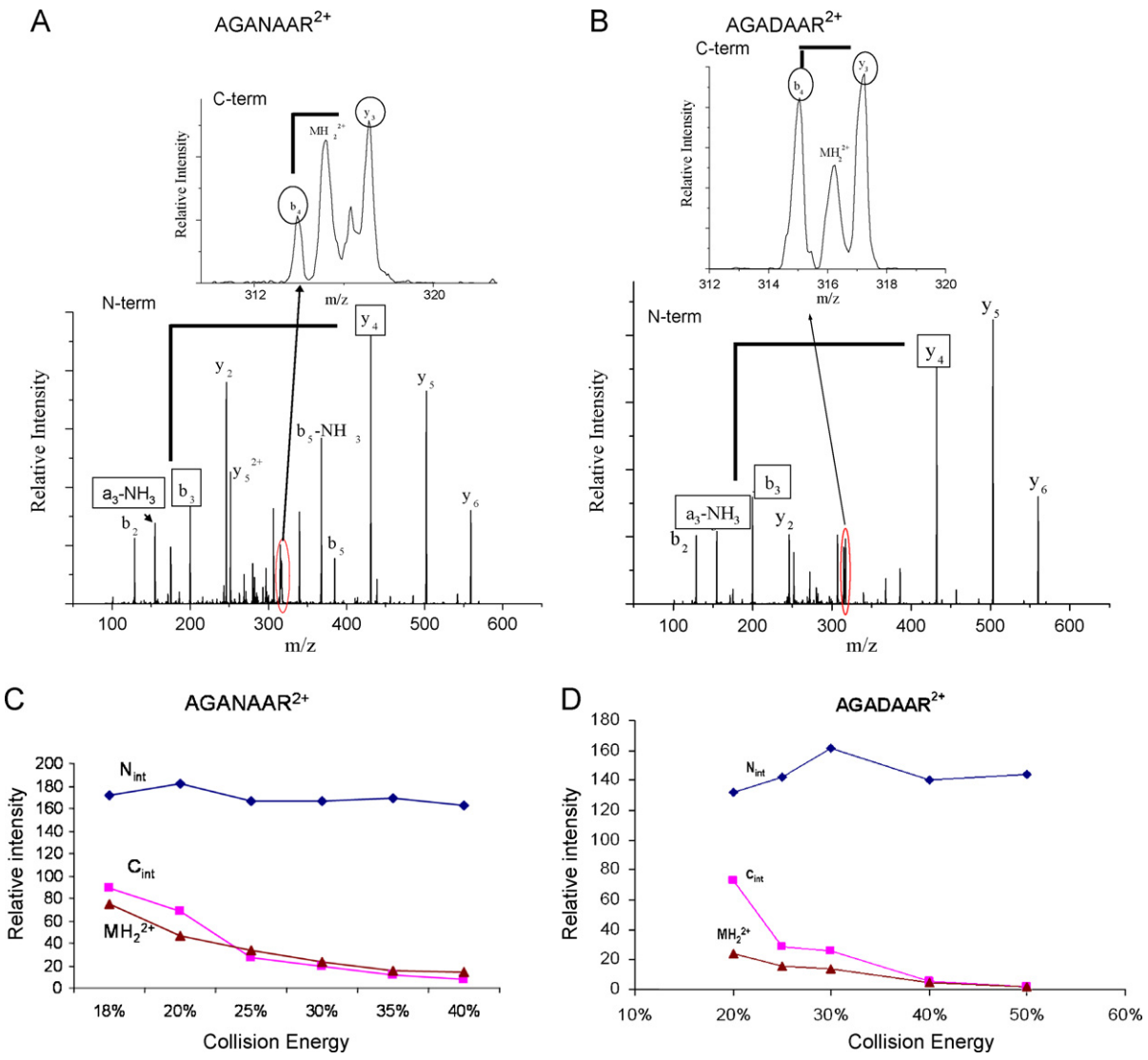

Fig. 4. The spectra of (A) doubly charged AGANAAR (*m*/*z*: 315.6) and (B) doubly charged AGADAAR (*m*/*z*: 316.2) by ESI/LCQ. The "% relative collision energy" (defined by the instrument manufacturer) used for acquiring the spectra was 20% for AGANAAR and 30% for AGADAAR. The circles denote fragments C-terminal to Asn/Asp and squares denote fragments N-terminal to Asn/Asp. Relative intensity curves for doubly charged (C) AGANAAR and (D) AGADAAR by LCQ/ESI. N_{int}: the intensity sum of fragments N-terminal to Asn/Asp, including y_4, b_3 and its secondary fragments (a_3 and a_3-NH_3) if observed. C_{int}: the intensity sum of fragments C-terminal to Asn/Asp, including y_3, b_4 and its secondary fragments (a_4 and a_4-NH_3) if observed. No obvious secondary fragmentation of y ions was observed.

further fragmentation of the y_3 peak (MS^3) were seen in either of the spectra, supporting the proposition that these features are primarily the result of selective cleavage processes. In contrast, CID of singly charged AGA**N**AAR produces a uniform cleavage pattern with extensive neutral loss of NH_3, while CID of singly charged AGA**D**AAR produces a preferential cleavage C-terminal to Asp which is expected and well-studied (data not shown) [35–37,39].

3.3. Explanation based on proton bridges

Ser, Thr, Cys, Asn, and Asp all show N-terminal enhanced cleavage, while Hse and Met both show C-terminal enhanced cleavages. The identity of the heteroatom within the side chain does not determine the fragmentation pattern; both oxygen- and sulfur-containing side chains demonstrate C-terminal or N-terminal enhanced cleavages. The length of the side chain for Ser, Thr, and Cys compared with Hse and Met differs by one methylene unit, possibly allowing for different hydrogen bonding or proton bridges to occur depending on the stability of the structures.

The fact that enhanced cleavage at these residues is only observed for doubly charged peptides indicates the involvement of an ionizing proton, which supports the possible formation of proton bridges between the side chain heteroatoms and backbone carbonyls. The formation of the proton bridge is also supported by previous studies in the literature, which showed that in the gas phase, the charge tends to be solvated by multiple heteroatoms [54,55]. The location and relative stability of these proton bridges could be the determining factor in whether the C-terminal cleavage or N-terminal cleavage is enhanced.

The possibility of forming proton bridges between amide nitrogens and the side chain hydroxyl is considered very low because of the low proton affinity of amide nitrogens in the gas phase. Calculations have shown that protonation at the carbonyl oxygen results in lower energy structures than protonation at the amide nitrogen [54,56]. For example, for dipeptides, the carbonyl oxygen-protonated structures are 56–71 kJ/mol lower in energy compared to the amide nitrogen-protonated structures [56].

For each of set of amino acids (Ser/Thr/Cys, Hse/Met, and Asp/Asn), the literature results for proton bridge stabilities will

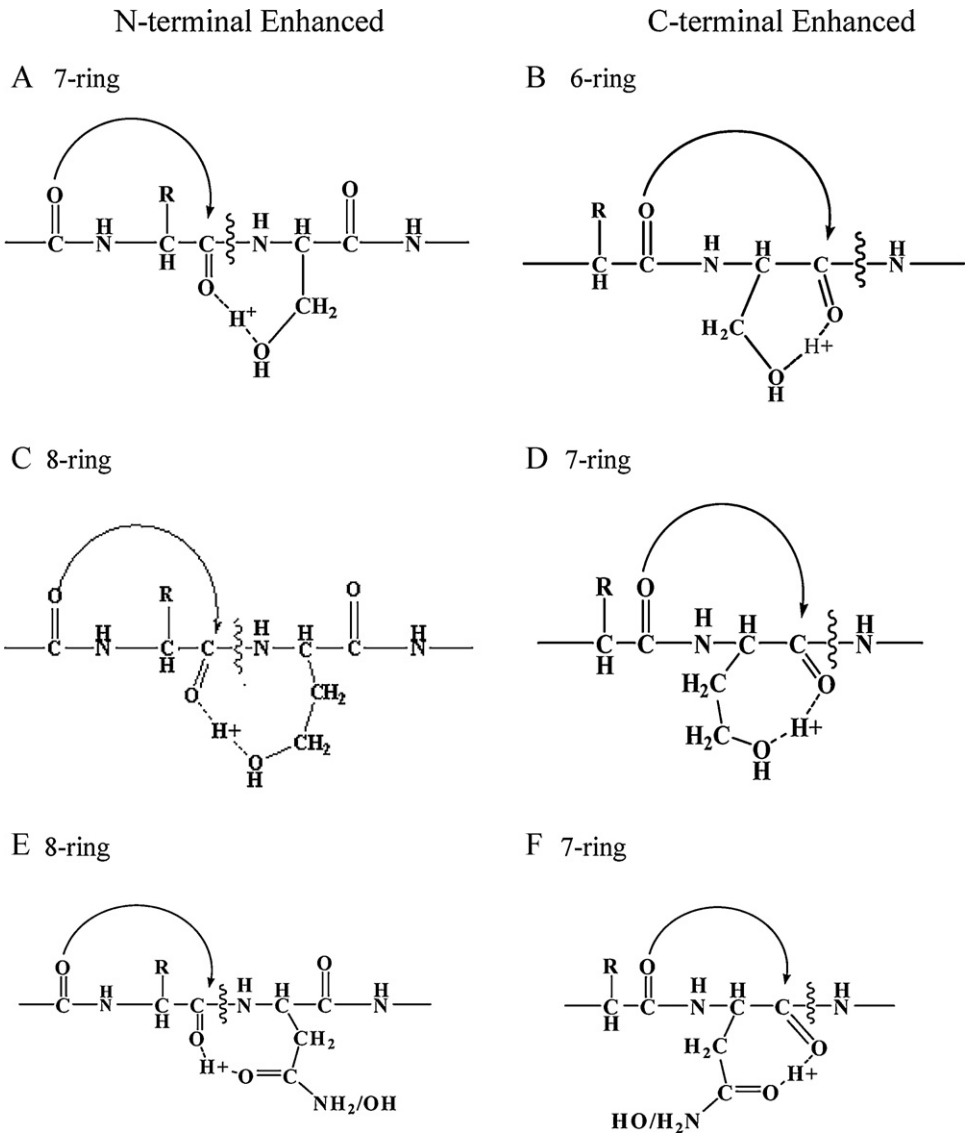

Fig. 5. Summary of proton bridge effects leading to N-terminal and C-terminal Enhanced Cleavages. (A) 7-membered ring between side chain hydroxyl and carbonyl N-terminal to Ser. (B) 6-membered ring between side chain hydroxyl and carbonyl C-terminal to Ser. (C) 8-membered ring formed between side chain hydroxyl and carbonyl N-terminal to Hse. (D) 7-membered ring between side chain hydroxyl and C-terminal carbonyl of Hse. (E) 8-membered ring between the side chain carbonyl and the carbonyl N-terminal to Asn/Asp. (F) 7-membered ring formed between side chain carbonyl and carbonyl C-terminal to Asn/Asp.

be discussed. Experimental and modeling results will also be presented that examine the proton bridge stability model.

3.4. Ser/Thr/Cys proton bridges: seven- vs. six-membered rings

Fig. 5A and B show two possible scenarios for the Ser side chain: the hydroxyl group can bridge a proton with the N-terminal carbonyl to form a seven-membered ring, or it can bridge a proton with the C-terminal carbonyl to form a six-membered ring. The difference in ring sizes for these two proton bridges causes a difference in the stability of these bridges. Szulejko et al. studied the stabilities of proton-bridged methoxyl alcohols with different ring sizes [57]. According to their study, the proton affinity of 4-methoxy-1-butanol, which forms a 7-membered cyclic proton bridge upon protonation is 918.4 kJ/mol. The proton affinity of 3-methoxy-1-propanol, which forms a 6-membered cyclic proton bridge, is 893.7 kJ/mol. This indicates that for proton bridges between hydroxyl/methoxyl groups, a 7-membered ring is more stable than a 6-membered ring.

Mautner's study also showed that for the proton bridge between two carbonyl groups, a 7-membered ring is more stable than a 6-membered ring [58]. As an example, the proton affinity of $CH_3COCH_2CH_2COCH_3$, which forms a 7-membered cyclic proton bridge upon protonation, is 885.50 kJ/mol as opposed to 868.76 kJ/mol, the proton affinity of $CH_3COCH_2COCH_3$ that forms a 6-membered cyclic proton bridge.

This is also consistent with Yamabe's studies on intramolecular proton bridges (X–H^+–X) of bifunctional molecules X–$(CH_2)_n$–X (X = –NH_2, –OR) [59]. According to this study, there is a good correlation between the hydrogen bond linearity and the stabilities of proton bridges for n = 2–4, which was confirmed by both ab inito calculations and experimental data. As n increases up to n = 4, the hydrogen bond X–H^+–X approaches a linear geometry, consequently resulting in increased stability for the proton bridge and an increased proton affinity of the molecule. When n = 4, a seven-membered ring is formed and the hydrogen bond angle is close to 180°, which makes it more stable than a six-membered cyclic proton bridge (n = 3).

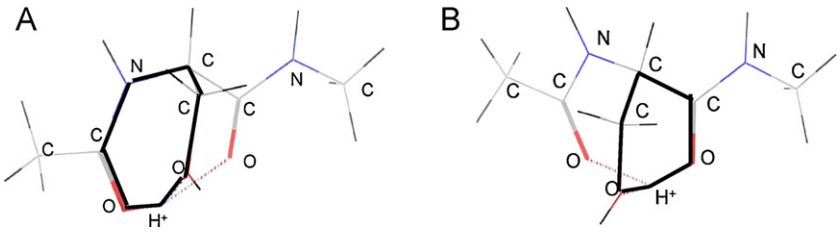

Fig. 6. The most stable structures of serine obtained by conformational searches (A) with proton on the carbonyl N-terminal to serine, (B) with proton on the carbonyl C-terminal to serine. Unlabeled atoms are hydrogen, black lines indicate ring containing proton bridge.

The studies by Szulejko, Mautner, and Yamabe all suggest that proton bridges can have a significant effect on the stability of a gas-phase conformation. Furthermore, they all demonstrate that a seven-membered ring would be more stable than a six-membered ring. For Ser, Thr, and Cys, a seven-membered ring could be formed between the heteroatom group of the Ser/Thr/Cys side chains and the N-terminal neighboring carbonyl. This would make the N-terminal carbonyl carbon more electro-positive and encourage the nucleophilic attack on that carbonyl carbon, thus promoting the formation of b/y ion pairs N-terminal to the amino acid in question. Both experimental and computational tests were undertaken in order to further probe this explanation.

Although in this paper we discussed nucleophilic attack by the adjacent carbonyl oxygen (as shown in Fig. 5) to form an oxazolone b_3 ion, we cannot rule out at least some percentage of structures formed by attack by the N-terminal amine to produce a cyclic tripeptide structure [60].

3.5. Fragmentation studies of side chain involvement

Although the stability of the resulting proton bridge could explain the enhanced cleavage effects that are observed, the presence of heteroatoms in the side chains of Ser, Thr, and Cys suggests another possibility for enhanced N-terminal cleavage in the spectra of the selected model peptides: the side chain might attack carbonyl on either side to form unconventional b and y ions. This mechanism, which has been reported for His and Asp, differs from the formation of typical oxazolone b and truncated peptide y ions, where the preceding backbone carbonyl oxygen attacks the carbonyl carbon at the cleaving amide bond [26]. In order to test this possibility, the b_3, y_4, b_4 and y_3 ions from doubly charged AGA**S**AAR were further fragmented and compared with the same ions from doubly charged AGA**A**AAR.

Further fragmentation of b_3 ions from AGA**S**AAR and AGA**A**AAR produces very similar spectra. Both b_3 ions produce a_3, which is expected for a b-type ion, and a_3-17, which has been reported as a prominent fragment for b_3 [61,62]. Further fragmentation of b_4 ions from AGA**S**AAR gives an intense b_4-H_2O peak, which is consistent with the presence of serine, but both b_4 ions produce an a_4 and a_4-NH_3 fragment. The MS^3 of y_3 ions from both AGA**S**AAR and AGA**A**AAR are very similar, both produce y_3-NH_3-H_2O and y_1 as dominant peaks. Further fragmentation of y_4 ions from AGA**S**AAR and AGA**A**AAR gives similar patterns with strong peaks at y_1, y_2-NH_3 and y_4-NH_3.

The b_3, y_4, b_4 and y_3 ions from AGA**A**AAR fragments can only form by typical backbone-initiated mechanisms because there are no side chains to initiate other types of cleavages. The similarity between the MS^3 fragmentation for AGA**A**AAR and AGA**S**AAR indicates that the b/y ions formed at serine are conventional b ions and y ions formed through typical fragmentation mechanisms not involving side chain attack. This is consistent with a calculation by Farrugia et al. that shows that the direct involvement of the serine side chain in forming a b-type ion is unfavorable [63]. Therefore the N-terminal enhancement observed at Ser, Thr, and Cys is not likely caused by the direct attack of the side chain. Molecular modeling was undertaken to assess the stability of potential proton bridged intermediates.

3.6. Molecular modeling of serine

MacroModel was used to perform molecular modeling on singly protonated CH_3CO-Ser-$NHCH_3$ to probe the location and stabilities of proton bridges involving Ser. The two carbonyl oxygens (N-acetyl and Ser) are the mostly likely protonation sites due to their high proton affinities relative to the amide nitrogen and the side chain hydroxyl oxygen. Structure A in Fig. 6 shows the most stable structure for protonation at the N-acetyl carbon, which is involved in two proton bridges—one to the Ser carbonyl and one to the side-chain hydroxyl oxygen. Structure B in Fig. 6 shows the most stable structure for protonation at the Ser carbonyl. Again, the Ser carbonyl is involved in two proton bridges—one to the N-acetyl carbonyl and one to the side-chain hydroxyl oxygen. Theory predicts that the 7-membered cyclic bridge between the N-acetyl carbonyl and the side chain hydroxyl will be more stable than the 6-membered cyclic bridge between the Ser carbonyl and the side chain hydroxyl.

Molecular dynamic simulations were performed separately on structures A and B to monitor the stability of the proton bridges. A temperature range from 300 K to 800 K was used, which corresponds to the expected energy deposition at different collision energies in an LCQ ion trap [64]. Table 1 shows the percentage of the carbonyl to side-chain proton bridge that remains at each temperature for structures A and B. As predicted by theory, the 7-membered cyclic bridge retained a higher percentage of the bridge compared to the 6-membered ring, showing a greater stability at the higher temperatures. The increased stability for the proton bridge between the N-acetyl carbonyl and the side chain hydroxyl oxygen also supports the experimental evidence for N-terminal enhanced cleavage (see Fig. 5A vs. B).

Although the overall percentage of proton bridges in B decreases, as expected with increased energy, the overall percentage in A actually increases. The structural strain involved in making two proton bridges may cause neither to be fully optimized in the original structure. The energy deposited during the molecular dynamic simulations can cause the less stable carbonyl–H^+–carbonyl proton bridge to break, releasing this structural strain and allowing the other proton bridge to optimize. This

Table 1
The percentage of remaining proton bridges among 10,000 structures at different temperatures for homoserine and serine.

	Ring size	300 K	500 K	800 K
CH_3CO-Ser-$NHCH_3$ (A)	7	51%	60%	70%
CH_3CO-Ser-$NHCH_3$ (B)	6	55%	46%	42%
CH_3CO-Hse-$NHCH_3$	7	45%	31%	44%
CH_3CO-Hse-$NHCH_3$	8	35%	32%	0

further indicates the stability of the 7-membered proton bridge, under the even more energetic conditions that exist during CID.

Although the most likely protonation site is the carbonyl oxygen, which has the highest proton affinity, the proton could also be transferred to hydroxyl group under the conditions of CID. Moreover, according to the literature, a proton an be sequestered by a site with a lower proton affinity to achieve an overall highly stable structure [65,66], which justifies the possible protonation of the serine side chain. To further probe the stabilities of 7- and 6-membered cyclic proton bridges under these conditions, the peptide AGA**S**AAR was built in MacroModel with the proton on the serine side chain hydroxyl group. When the proton is on the serine side chain, the most stable structure obtained from a conformational search has two hydrogen bonds from the hydroxyl hydrogen on the serine side chain bridging to the N-acetyl carbonyl (7-membered ring) and another one bridging to the Ser carbonyl (6-membered ring). A molecular dynamics study was performed at a representative temperature of 500 K. The results show that the hydrogen bond to the N-acetyl carbonyl at serine is more stable: among 10,000 sampled structures, 98.5% of the structures retain the proton bridge to the N-terminal carbonyl compared to the proton bridge to the Ser carbonyl, which was retained in only 44.8% of the structures.

The above molecular dynamics results suggest that the 7-membered cyclic proton bridge from the Ser side chain to the adjacent N-acetyl carbonyl is more stable than the 6-membered cyclic proton bridge to the Ser carbonyl. This confers electropositive character on the carbonyl N-terminal to Ser in a peptide, providing an explanation for enhanced cleavage N-terminal to Ser. This stability is consistent with N-terminal enhanced cleavage at Ser as discussed above. The same explanation can be applied to threonine and cysteine.

3.7. Hse/Met proton bridges: seven- vs. eight-membered ring

Homoserine and methionine have similar side chain heteroatoms compared to Ser, Thr, and Cys, but they both demonstrate enhanced cleavage at the C-terminus. This behaviour can also be explained by exploring proton bridge stabilities. Hse and Met have one extra methylene group in their side chains compared to Ser, Thr, and Cys, so a proton bridge between the side chain and the N-terminal carbonyl oxygen forms an 8-membered ring. In the case of Hse (Fig. 5C and D) and Met, a 7-membered proton bridge is formed between the side chain and the C-terminal carbonyl.

Several lines of evidence in the literature show that a 7-membered cyclic proton bridge is more stable than an 8-membered cyclic proton bridge. According to Szulejko's study [57], the proton affinities ($-\Delta H$) of methoxyl alcohols with the 7- and 8-membered cyclic proton bridges are very close: 219.8 and 219.4 kcal/mol, respectively. However, the entropy changes (ΔS) for the formation of 7- and 8-membered rings are different, which leads to differences in gas phase basicities ΔG [57]. The difference in ΔS for the formation of 7- and 8-membered cyclic proton bridge is 3.4 cal mol^{-1}·K^{-1} (with the 7-membered cyclic one at -15.8 cal mol^{-1}·K^{-1} and the 8-membered cyclic one at -19.2 cal mol^{-1}·K^{-1} when pyrrole is used as reference base). In other words, the entropy change favors the 7-membered cyclic proton bridge vs. the 8-membered cyclic proton bridge. The entropy effect becomes the deciding factor with the effective temperatures at several hundred degrees ($\Delta G = \Delta H - T\Delta S$). A proton bridge with the adjacent C-terminal carbonyl oxygen causes the C-terminal carbonyl carbon to become more electropositive. This facilitates the nucleophilic attack presumably by the preceding electronegative carbonyl oxygen, and results in the enhanced cleavage C-terminal to homoserine and methionine (Fig. 5D).

3.8. Molecular modeling of Hse and Met

Molecular dynamics were performed to probe the stabilities of the proton bridges for homoserine. A simplified structure CH_3CO-Hse-$NHCH_3$ was built in MacroModel, and the ionizing proton was put on each of the two carbonyl oxygens to form two different protonated structures. A conformational search was performed for these two different structures separately to obtain their most stable structures. Results show their most stable structures contain the proton bridge between the hydroxyl group and either the N-acetyl or Hse carbonyl depending on the different protonation sites. These structures were subjected to molecular dynamics modeling (Table 1). It was shown that, among 10,000 sampled structures for each structure, 45.1% of the 7-membered ring structures retain the proton bridge at temperature 300 K, while only 34.6% of the 8-membered ring structures retain the proton bridge at the same temperature. At 800 K, 43.6% of the 7-membered ring structures retain the proton bridge, while none of the 8-membered ring proton bridge is retained. This demonstrates the higher stability of the 7-membered cyclic proton bridge compared to the 8-membered cyclic one.

3.9. Asn/Asp proton bridges

For Asn and Asp-containing peptides, enhanced cleavage N-terminal to Asn/Asp only occurs for doubly charged peptides and not singly charged peptides; this points to the involvement of an ionizing proton, which supports the formation of proton bridges between the side chain carbonyls and backbone carbonyls. If the carbonyl oxygens of the side chains are involved in the proton bridge, then two possible bridges can be formed: an 8-membered proton bridge would form between the side chain and the N-terminal carbonyl, or a 7-membered proton bridge would form between the side chain and the C-terminal carbonyl (Fig. 5E and 5F). While a 7-membered cyclic proton bridge is the most stable bridge between an –OH or –SH side chain and a carbonyl, the case is different for proton bridges between two amide carbonyl groups. Witt and Grutzmacher [67] investigated the effect of ring size on the stability of proton bridges between two carbonyl oxygens involved in amide bonds. According to their results, the enthalpy release (ΔH) of an 8-membered cyclic proton bridge between two carbonyls is 27 kJ/mol (6.46 kcal/mol) higher than that of a 7-membered cyclic proton bridge. While entropy favors the formation of a 7-membered ring, the difference in entropy ($\Delta S = 0.024$ kJ/mol·K) is small compared to the enthalpy. Based on these results, an 8-membered cyclic proton bridge would be favored between two amide carbonyl oxygens.

For Asn and Asp, an 8-membered cyclic proton bridge between the side-chain carbonyl and the N-terminal backbone carbonyl would be more stable than with the C-terminal carbonyl. Presumably the formation of the 8-membered ring makes the carbonyl carbon N-terminal to Asn/Asp (Fig. 5E) more electropositive and susceptible to attack, leading to the enhanced cleavage N-terminal to Asn or Asp.

Fragmentation of doubly charged AGAEAAR and AGAQAAR has also been performed, and no obvious enhanced cleavage was observed, which is presumably due to the high entropy cost of forming a 9-membered cyclic proton bridge between the side chain and the N-terminal carbonyls.

3.10. Fragmentation studies of side chain involvement for Asn/Asp

As in the case of Ser, the side chain could also be involved in initiating the cleavage. To investigate possible side chain involvement in initiating the cleavage C-terminal to Asn and Asp, b_4 ions from the doubly and singly charged AGA**N**AAR/AGA**D**AAR were fragmented.

In parallel with the MS^3 data described for Ser, no obvious evidence of side chain involvement was found for doubly charged AGA**N**AAR/AGA**D**AAR. The b_4 from singly charged AGA**D**AAR, however, produces a peak at b_4-72 (b_4-CO_2-CO) as reported [35] consistent with an anhydride structure and the involvement of side chain in initiating the formation of b_4.

4. Conclusions

A series of doubly charged synthetic model peptides shows stronger cleavages N-terminal to Ser, Thr, Asn and Asp and C-terminal to homoserine and Met in comparison with cleavages at the opposite termini of these residues. The relationship between the chemical properties of the amino acids and their characteristic fragmentation patterns was investigated. It is proposed that proton bridges form between side chain heteroatoms and neighboring carbonyl oxygens. The proton bridged structures will have different ring sizes depending on whether the proton bridge is formed between the N-terminal carbonyl and the side chain or the C-terminal carbonyl and the side chain. The enhanced cleavages result from the different stabilities of the proton bridges at different ring sizes. Molecular dynamics modeling was performed to probe the stabilities of different proton bridges.

Proton bridges between side chain hydroxyl/thiol and backbone carbonyls:

(a) For serine, threonine and cysteine, a 7-membered cyclic proton bridge between the side chain heteroatom and the protonated carbonyl N-terminal to these residues is more stable than the 6-membered cyclic proton bridge between the side chain and the carbonyl C-terminal to these residues. This leads to enhanced cleavages N-terminal to these residues by making the carbonyl on the N-terminal side more electropositive and encouraging nucleophilic attack on that carbonyl.
(b) For homoserine and methionine, an 8-membered ring is formed if the proton bridge is between the side chain and the carbonyl N-terminal to the residue, and a 7-membered ring if the proton bridge is between the side chain and the carbonyl C-terminal to these residues. The 7-membered cyclic proton bridge is entropically favored and thus more stable compared to the 8-membered proton bridge, which leads to the enhanced cleavages C-terminal to homoserine and methionine.

Proton bridges between the side chain carbonyl and backbone carbonyls:

For asparagine and aspartic acid, an 8-membered ring that bridges by a proton between the side chain carbonyl and the carbonyl on the N-terminal side of Asp/Asn is more stable than a 7-membered ring between the side chain carbonyl and the carbonyl C-terminal to Asp/Asn, which explains the enhancement of cleavages N-terminal to Asp/Asn for doubly charged peptides.

Acknowledgments

This work was supported by NIH grant GMR0151387 awarded to Dr. Vicki H. Wysocki. B.P. was supported in part by NIH grant T32 GM08804.

References

[1] J.B. Fenn, M. Mann, C.K. Meng, S.F. Wong, C.M. Whitehouse, Electrospray ionization for mass-spectrometry of large biomolecules, Science (Washington, DC) 246 (1989) 64–71.
[2] M. Karas, A. Ingendoh, U. Bahr, F. Hillenkamp, Ultraviolet-laser desorption ionization mass-spectrometry of femtomolar amounts of large proteins, Biomedical & Environmental Mass Spectrometry 18 (1989) 841–843.
[3] K. Tanaka, H. Waki, Y. Ido, S. Akita, Y. Yoshida, T. Yohida, Protein polymer analyses up to *m*/*z* 100,000 by laser ionization time-of-flight mass spectrometry, Rapid Communications in Mass Spectrometry 2 (1988) 151–153.
[4] J. Bergquist, FTICR mass spectrometry in proteomics, Current Opinion in Molecular Therapeutics 5 (2003) 310–314.
[5] P. Juhasz, J.M. Campbell, M.L. Vestal, MALDI-TOF/TOF technology for peptide sequencing and protein identification, Mass Spectrometry and Hyphenated Techniques in Neuropeptide Research (2002) 375–413.
[6] R.J. Cotter, The new time-of-flight mass spectrometry, Analytical Chemistry (1999) 445A–451A.
[7] R.E. March, Quadrupole ion trap mass spectrometer, in: R.A. Meyers (Ed.), Encyclopedia of Analytical Chemistry, John Wiley and Sons Ltd., Chichester, 2000, pp. 11848–11872.
[8] P.E Miller, B.M. Denton, The quadruple mass filter: basic operating concepts, Journal of Chemical Education (1986) 617.
[9] I.V. Chernushevich, A.V. Loboda, B.A. Thomson, An introduction to quadrupole-time-of-flight mass spectrometry, Journal of Mass Spectrometry 36 (2001) 849–865.
[10] J.E.P. Syka, J.A. Marto, D.L. Bai, S. Horning, M.W. Senko, J.C. Schwartz, B. Ueberheide, B. Garcia, S. Busby, T. Muratore, J. Shabanowitz, D.F. Hunt, Novel linear quadrupole ion trap/FT mass spectrometer: performance characterization and use in the comparative analysis of histone H3 post-translational modifications, Journal of Proteome Research 3 (2004) 621–626.
[11] C. Gu, A. Somogyi, V.H. Wysocki, K.F. Medzihradszky, Fragmentation of protonated oligopeptides XLDVLQ [X = L, HK or R] by surface induced dissociation: additional evidence for the 'mobile proton' model, Analytica Chimica Acta 397 (1999) 247–256.
[12] H.J. Cooper, K. Hakansson, A.G. Marshall, The role of electron capture dissociation in biomolecular analysis, Mass Spectrometry Reviews 24 (2005) 201–222.
[13] J.E.P. Syka, J.J. Coon, M.J. Schroeder, J. Shabanowitz, D.F. Hunt, Peptide and protein sequence analysis by ETD-MS, Proceedings of the National Academy of Sciences of the United States of America 101 (2004) 9528–9533.
[14] R.S. Johnson, S.A. Martin, K. Biemann, Collision-induced fragmentation of $[M+H]^+$ ions of peptides side chain specific sequence ions, International Journal of Mass Spectrometry and Ion Processes 86 (1988) 137–154.
[15] W.J. Henzel, T.M. Billeci, J.T. Stults, S.C. Wong, C. Grimely, C. Watanabe, Identifying proteins from 2-dimensional gels by molecular mass searching of peptide fragments in protein sequence databases, Proceedings of the National Academy of Sciences of the United States of America 90 (1993) 5011–5015.
[16] W.J. Henzel, C. Watanabe, J.T. Stults, Protein identification: the origins of peptide mass fingerprinting, Journal of the American Society for Mass Spectrometry 14 (2003) 931–942.
[17] J.R. Yates, S. Speicher, P.R. Griffin, T. Hunkapiller, Peptide mass maps: a highly informative approach to protein identification, Analytical Biochemistry 214 (1993) 397–408.
[18] M. Mann, P. Hoejrup, P. Roepstorff, Use of mass spectrometric molecular weight information to identify proteins in sequence databases, Biological Mass Spectrometry 22 (1993) 338–345.
[19] J.K. Eng, A.L. McCormack, J.R. Yates III, An approach to correlate tandem mass spectral data of peptides with amino acid sequences in a protein database, Journal of the American Society for Mass Spectrometry 5 (1994) 976–989.
[20] D.N. Perkins, D.J.C. Pappin, D.M. Creasy, J.S. Cottrell, Probability based protein identification by searching sequence databases using mass spectrometry data, Electrophoresis 20 (1999) 3551–3567.
[21] R. Craig, R.C. Beavis, Tandem: matching proteins with tandem mass spectra, Bioinformatics 20 (2004) 1466–1467.
[22] R. Craig, R.C. Beavis, Peaks: powerful software for peptide de novo sequencing by MS/MS, Rapid Communications in Mass Spectrometry 17 (2003) 2310–2316.
[23] L.Y. Geer, S.P. Markey, J.A. Kowalak, L. Wagner, M. Xu, D.M. Maynard, X. Yang, W. Shi, S.H. Bryant, Open mass spectrometry search algorithm, Journal of Proteome Research 5 (2004) 958–964.
[24] J. Colinge, A. Masselot, M. Giron, T. Dessingy, J. Magnin, OLAV: towards high-throughput tandem mass spectrometry data identification, Proteomics 3 (2003) 1454–1463.
[25] A.R. Dongre, J.L. Jones, A. Somogyi, V.H. Wysocki, Influence of peptide composition gas-phase basicity, and chemical modification on fragmentation efficiency: evidence for the mobile proton model, Journal of the American Chemical Society 118 (1996) 8365–8374.
[26] V.H. Wysocki, G. Tsaprailis, L.L. Smith, L.A. Breci, Mobile and localized protons: a framework for understanding peptide dissociation, Journal of Mass Spectrometry 35 (2000) 1399–1406.
[27] I.A. Papayannopoulos, The interpretation of collision induced dissociation tandem mass spectra of peptides, Mass Spectrometry Reviews 14 (1995) 49–73.
[28] K.A. Cox, S.J. Gaskell, M. Morris, A. Whiting, Role of the site of protonation in the low-energy decompositions of gas-phase peptide ions, Journal of the American Society for Mass Spectrometry 7 (1996) 522–531.
[29] T. Wyttenbach, G. von Helden, M.T. Bowers, Gas-phase conformation of biological molecules: bradykinin, Journal of the American Chemical Society 118 (1996) 8355–8364.
[30] K.M. Downard, K. Biemann, Charging behavior of highly basic peptides during electrospray ionization. A predilection for protons, International Journal of Mass Spectrometry and Ion Processes 148 (1995) 191–202.
[31] X.J. Tang, P. Thibault, R.K. Boyd, Fragmentation reactions of multiply-protonated peptides and implications for sequencing by tandem mass-spectrometry with low-energy collision-induced dissociation, Analytical Chemistry 65 (1993) 2824–2834.

[32] A.R. Dongre, A. Somogyi, V.H. Wysocki, Surface-induced dissociation: an effective tool to probe structure, energetics and fragmentation mechanisms of protonated peptides, Journal of Mass Spectrometry 31 (1996) 339–350.
[33] S.G. Summerfield, A. Whiting, S.J. Gaskell, Intra-ionic interactions in electrosprayed peptide ions, International Journal of Mass Spectrometry and Ion Processes 162 (1997) 149–161.
[34] G. Tsaprailis, H. Nair, W. Zhong, K. Kuppannan, J.H. Futrell, V.H. Wysocki, A mechanistic investigation of the enhanced cleavage at histidine in the gas-phase dissociation of protonated peptides, Analytical Chemistry 76 (2004) 2083–2094.
[35] C. Gu, G. Tsaprailis, L. Breci, V.H. Wysocki, Selective gas-phase cleavage at the peptide bond C-terminal to aspartic acid in fixed-charge derivatives of Asp-containing peptides, Analytical Chemistry 72 (2000) 5804–5813.
[36] G. Tsaprailis, A. Somogyi, E.N. Nikolaev, V.H. Wysocki, Refining the model for selective cleavage at acidic residues in arginine-containing protonated peptides, International Journal of Mass Spectrometry 195–196 (2000) 467–479.
[37] Y. Huang, J.M. Triscari, G.C. Tseng, M.S. Pasa-Tolic, R.D. Smith, V.H. Wysocki, Statistical characterization of the charge state and residue dependence of low-energy CID peptide dissociation patterns, Analytical Chemistry 77 (2005) 5800–5813.
[38] L.A. Breci, D.L. Tabb, J.R. Yates III, V.H. Wysocki, Cleavage N-terminal to proline: analysis of a database of peptide tandem mass spectra, Analytical Chemistry 75 (2003) 1963–1971.
[39] Y. Huang, J.M. Triscari, L. Pasa-Tolic, G.A. Anderson, M.S. Lipton, R.D. Smith, V.H. Wysocki, Dissociation behavior of doubly-charged tryptic peptides: correlation of gas-phase cleavage abundance with Ramachandran plots, Journal of the American Chemical Society 126 (2004) 3034–3035.
[40] D.L. Tabb, L.L. Smith, L.A. Breci, V.H. Wysocki, D. Lin, J.R. Yates III, Statistical characterization of ion trap tandem mass spectra from doubly charged tryptic peptides, Analytical Chemistry 75 (2003) 1155–1163.
[41] A. Frank, P. Pevzner, PepNovo: de novo peptide sequencing via probabilistic network modeling, Analytical Chemistry 77 (2005) 964–973.
[42] E. Atherton, R.C. Sheppard, Fluorenylmethoxycarbonyl-polyamide solid phase peptide synthesis—general principles and development, in: Solid-Phase Peptide Synthesis: A Practical Approach, IRL Press at Oxford University Press, Oxford, UK, 1989.
[43] T. Yalcin, I.G. Csizmadia, M.R. Peterson, A.G. Harrison, The structure and fragmentation of B_n [$n \geq 3$] ions in peptide spectra, Journal of the American Society for Mass Spectrometry 7 (1996) 233–242.
[44] T. Yalcin, C. Khouw, I.G. Csizmadia, M.R. Peterson, A.G. Harrison, Why are B ions stable species in peptide spectra? Journal of the American Society for Mass Spectrometry 6 (1995) 1165–1174.
[45] M.J. Nold, C. Wesdemiotis, T. Yalcin, A.G. Harrison, Amide bond dissociation in protonated peptides. Structures of the N-terminal ionic and neutral fragments, International Journal of Mass Spectrometry and Ion Processes 164 (1997) 137–153.
[46] B. Paizs, G. Lendvay, K. Vwkey, S. Suhai, Formation of b2 + ions from protonated peptides: an ab initio study, Rapid Communications in Mass Spectrometry 13 (1999) 525–533.
[47] U. Erlekam, B.J. Bythell, D. Scuderi, M. Van Stipdonk, B. Paizs, P. Maitre, Infrared spectroscopy of fragments of protonated peptides: direct evidence for macrocyclic structures of b5 ions, Journal of the American Chemical Society 131 (32) (2009) 11503–11508.
[48] P. Roepstorff, Letter to the editors, Biomedical Mass Spectrometry 11 (1984) 601.
[49] R.S. Johnson, S.A. Martin, K. Biemann, J.T. Stults, J.T. Watson, Novel fragmentation process of peptides by collision-induced decomposition in a tandem mass spectrometer: differentiation of leucine and isoleucine, Analytical Chemistry 59 (1987) 2621–2625.
[50] A.T. Iavarone, E.R. Williams, Collisionally activated dissociation of supercharged proteins formed by electrospray ionization, Analytical Chemistry 75 (2003) 4525–4533.
[51] H. Nair, V.H. Wysocki, Are peptides without basic residues protonated primarily at the amino terminus? International Journal of Mass Spectrometry and Ion Processes 174 (1998) 95–100.
[52] R.L. Beardsley, J.P. Reilly, Fragmentation of amidinated peptide ions, Journal of the American Society for Mass Spectrometry 15 (2004) 158–167.
[53] D.L. Tabb, Y. Huang, V.H. Wysocki, J.R. Yates III, Influence of basic residue content on fragment ion peak intensities in low-energy collision-induced dissociation spectra of peptides, Analytical Chemistry 76 (2004) 1243–1248.
[54] C.F. Rodriquez, A. Cunje, T. Shoeib, I.K. Chu, A.C. Hopkinson, K.W.M. Siu, Proton migration and tautomerism in protonated triglycine, Journal of the American Chemical Society 123 (2001) 3006–3012.
[55] J. Wu, C.B. Lebrilla, Gas-phase basicities and sites of protonation of glycine oligomers [GLY; n = 1–5], Journal of the American Chemical Society 115 (1993) 3270–3275.
[56] B. Paizs, M. Schnoelzer, U. Warnken, S. Suhai, A.G. Harrison, Cleavage of the amide bond of protonated dipeptides, Physical Chemistry Chemical Physics 6 (2004) 2691–2699.
[57] J.E. Szulejko, T.B. McMahon, V. Troude, G. Bouchoux, H.E. Audier, Structure and energetics of protonated ω-methoxy alcohols, Journal of Physical Chemistry A 102 (1998) 1879–1887.
[58] M. Meot-Ner, The ionic hydrogen bond. 2. Intramolecular and partial bonds. Protonation of polyethers, crown ethers, and diketones, Journal of the American Chemical Society 105 (1983) 4906–4911.
[59] S. Yamabe, K. Hirao, H. Wasoda, A correlation between proton affinities and intramolecular hydrogen bonds in bifunctional organic compounds, Journal of Physical Chemistry 96 (1992) 10261–10264.
[60] X.A. Chen, J.D. Steill, J. Oomens, N.C. Pollfer, Oxazolone versus macrocycle structures for Leu-enkephalin b(2)-b(4): insights from infrared multiple-photon dissociation spectroscopy and gas-phase hydrogen/deuterium exchange, Journal of the American Society for Mass spectrometry 21 (2010) 1313–1321.
[61] A.G. Harrison, A.B. Young, Fragmentation of protonated oligoalanines: amide bond cleavage and beyond, Journal of the American Society for Mass Spectrometry 15 (2004) 1810–1819.
[62] T. Cooper, E. Talaty, J. Grove, M. Van Stipdonk, S. Suhai, B. Paizs, Isotope labeling and theoretical study of the formation of a3* ions from protonated tetraglycine, Journal of the American Society for Mass Spectrometry 17 (2006) 1654–1664.
[63] J.M. Farrugia, R. O'Hair, G.E. Reid, Do all b_2 ions have oxazolone structures? Results from multistage mass spectrometry and ab initio studies on protonated N-acyl amino acid model systems, International Journal of Mass Spectrometry 210/211 (2001) 71–87.
[64] D.E. Goeringer, K.G. Asano, S.A. McLuckey, Ion internal temperature and ion trap collisional activation: protonated leucine enkephalin, International Journal of Mass Spectrometry 182/183 (1999) 275–288.
[65] C.A. Deakyne, M. Meot-Ner, C.L. Campbell, M.G. Hughes, S.P. Murphy, Multicomponent cluster ions. I. The proton solvated by CH_3CN/H_2O, Journal of Chemical Physics 84 (1986) 4958–4969.
[66] S. Wei, W.B. Tzeng, R.G. Keesee, A.W. Castleman Jr., Metastable unimolecular and collision-induced dissociation of hydrogen-bonded clusters: evidence for intracluster molecular rearrangement and the structure of solvated protonated complexes, Journal of the American Chemical Society 113 (1991) 1960–1969.
[67] M. Witt, H.-F. Grutzmacher, Effects of internal hydrogen bonds between amide groups: gas-phase basicity and proton affinity of linear aliphatic dicarboxamides, European Journal of Mass Spectrometry 6 (2000) 97–107.